The quantitative importance of key root traits for radial water loss under low water potential

Zhiwei Song · **Francesco Zonta** · **Lucas León Peralta Ogorek** ·
Viggo Klint Bastegaard · **Max Herzog** · **Elisa Pellegrini** · **Ole Pedersen**

Abstract

Aims Root tissue water can be lost to the dry topsoil via radial water loss (RWL) resulting in root shrinking and loss of contact with the rhizosphere. The root barrier to radial oxygen loss (ROL) has been shown to restrict RWL, therefore we hypothesized that the inducible barrier can be formed as a response to low soil water potential and play a role, together with other root traits, in restricting RWL.

Methods Rice and wheat were grown in hydroponics with contrasting water potential to diagnose ROL barrier formation and to explore how key root traits

(ROL barrier, root diameter, root porosity) affect RWL. Moreover, we developed a numerical model predicting RWL as a function of root diameter, root porosity and presence of a barrier to ROL.

Results Methylene blue staining showed that low water potential induced a ROL barrier formation in roots of rice, and also resulted in an apoplastic barrier, as identified by the apoplastic tracer periodic acid. The barrier significantly restricted RWL, but root diameter and tissue porosity also influenced RWL. Our numerical model was able to reflect the empirical data and clearly demonstrated that thick roots and a barrier to ROL restricts RWL while cortical porosity accelerates RWL.

Conclusions Our modelling approach highlighted that increase in root tissue porosity, a common response to drought, conserves water when new roots are formed, but the higher desiccation risk related to high-porosity roots can be effectively counteracted by forming thick roots or even better, by a barrier to ROL.

Zhiwei Song and Francesco Zonta contributed equally to this work.

Z. Song · L. L. P. Ogorek · V. K. Bastegaard · M. Herzog · E. Pellegrini (✉) · O. Pedersen (✉)
The Freshwater Biological Laboratory, Department of Biology, University of Copenhagen, Universitetsparken 4, 3rd Floor, 2100 Copenhagen, Denmark
e-mail: elisa.pellegrini@uniud.it

O. Pedersen
e-mail: opedersen@bio.ku.dk

F. Zonta
Institute of Fluid Mechanics and Heat Transfer, TU-Wien, 1060 Vienna, Austria

E. Pellegrini
Department of Food, Agricultural, Environmental and Animal Sciences, University of Udine, via delle Scienze 206, Udine, Italy

O. Pedersen
School of Agriculture and Environment, The University of Western Australia, 35 Stirling Highway, Crawley, WA 6009, Australia

Introduction

Variations in climatic conditions remain crucial in controlling crop yields. In substantial areas of the world, more than 60% of rice, maize, wheat and soybean yield variability is explained by year-to-year climate variability (Ray et al. 2015). In addition, IPCC projects that climate extremes, such as droughts and floods, will result in future global yield declines even if global warming is limited to 1.5–2 °C (Hoegh-Guldberg et al. 2018). Crop varieties with enhanced tolerance to abiotic stress can mitigate these negative effects of extreme weather events (Dhankher and Foyer 2018). This calls for a second Green Revolution by focusing on root traits that allow efficient soil resource capture (Lynch 2007). Drought severely impacts crop yields as water deficiency at the shoot level leads to stomatal closure and reduced photosynthesis (Leng and Hall 2019). Moreover, roots may lose water via radial water loss (RWL) resulting in cell death if roots desiccate entirely (Stasovski and Peterson 1993). We therefore aimed at quantifying the importance of the root apoplastic barriers and other root traits (e.g. aerenchyma, stele area, root diameter) on root RWL. Here we show that thick roots and modifications in the exodermis both work in concert to reduce RWL, whereas aerenchyma increases RWL.

As sessile organisms, plants cope with droughts via several key root traits with different trade-offs (Comas et al. 2013). Aerenchyma formation in maize has been shown to improve drought tolerance by decreasing root metabolic costs, permitting greater root growth and water uptake from dry soil (Klein et al. 2020; Zhu et al. 2010). However, aerenchyma formation has also been shown to impede movement of water through the root cortex in rice (Yang et al. 2012). In addition, thin roots are generally viewed as advantageous under drought conditions as exemplified in rice, where 8 genotypes of lowland rice all responded to water stress by a significant reduction in diameter of the nodal roots (Azhiri-Sigari et al. 2000). Thin roots increase the volume of soil that can be explored for

water, since much longer roots can be formed with the same investment in resources, and thin roots also increase the surface area in contact with the soil (Comas et al. 2013). Meanwhile, desiccation increases the strength of many agricultural soils, and thicker roots have been shown to have greater penetration ability in hard soils, as they are more resistant to buckling and deflection (Lynch et al. 2021). Research generally supports that plants with large diameter xylem vessels have greater hydraulic conductivity, but less conservative water use ("water banking") and greater risk of cavitation than those with small diameter vessels. However, exceptional species with large xylem diameters resistant to cavitation have been found, and large xylem diameters may be advantageous if water is ample at depth. The cortex to stele ratio (CSR) was found to increase with soil water content (i.e., stele area increased with declining water availability) in 18 wild Poaceae species (Yamauchi et al. 2021b). In addition, drought may also cause root shrinkage, and thereby reduce the root-soil contact surface. For example, in spruce species (*Picea abies* L. Karst), root circularity decreased in dry soils, and drought-tolerant species maintained higher root circularity than drought-sensitive species (Wrońska-Wałach et al. 2016). Water loss from roots has been related to the deposition of suberin and lignin in the exodermis restricting radial water loss (Cruz et al. 1992; Enstone et al. 2003). I.e., RWL from roots of plant species without an exodermal barrier was much higher than that in species with a well-developed exodermis (Cruz et al. 1992; Taleisnik et al. 1999). The many trade-offs in the above listed traits therefore call for a quantitative approach using mathematical modelling evaluating pros and cons of each trait.

Interestingly, flood tolerant species also develop some of the above-mentioned traits involved in drought tolerance. As soil flooding leads to depletion of oxygen available for root respiration (Drew 1992; Hepworth et al. 2015), wetland plants tolerate soil flooding via various root traits including aerenchyma formation (Pedersen et al. 2021b; Yamauchi et al. 2021a, b). These interconnected gas spaces in the root cortex result in a high capacity for oxygen diffusion to root apices during soil flooding, supporting mitotic cell divisions leading to root growth (Mano et al. 2006). A high CSR in

roots is beneficial for oxygen diffusion along roots in soil flooding, as a thin stele and large cortex allow for more aerenchyma to develop (Yamauchi et al. 2019). Importantly, roots of some wetland plants can form a barrier to radial oxygen loss (ROL) to alleviate hypoxia caused by soil flooding (Pedersen et al. 2021b). A barrier to ROL caused by suberin and lignin deposition in the exodermis of the basal root zones can enhance longitudinal oxygen diffusion in the aerenchyma by restricting oxygen loss to the rhizosphere (Colmer 2003). The barrier to ROL in roots of rice can be induced by growth in stagnant, deoxygenated nutrient solution (Colmer et al. 1998) and by various environmental signals such as low molecular carboxylic acids (Colmer et al. 2019) and reduced iron (Mongon et al. 2014) and it can be further strengthened by sulphide (Armstrong and Armstrong 2005). In addition, the barrier to ROL can impede the apoplastic entry of iron into the roots of *Urochloa humidicola* (Jimenez et al. 2021), but also to some extent reduce water uptake in wheat and rice roots (Ouyang et al. 2020).

The above clearly shows that some root traits appear as dual-purpose traits, including for both flood and drought tolerance. This is true for aerenchyma formation in particular, which formed substantially in plants growing in dry as well as in wet soils, while forming much less at intermediate soil water content (Yamauchi et al. 2021b). In addition, the ROL barrier forming in roots of plants exposed to waterlogging also restricts radial water loss (Peralta Ogorek et al. 2021). Since ROL and RWL in roots both seem related to the formation of a barrier in the exodermis (Taleisnik et al. 1999; Toulotte et al. 2022), the present study tested the hypothesis that a root barrier to ROL is formed as a response to drought using hydroponics, where the water potential of the nutrient solution was manipulated with PEG-6000. Moreover, we used a mathematical modelling approach to illustrate the quantitative importance of key root traits (root barrier to ROL, root porosity and root diameter) on radial water loss. The modelling approach used input data from roots of rice and wheat (in order to achieve a wide range in the included root traits) and also artificial roots made from agar cylinders (in order to assess the effect of root diameter without confounding influence from other root traits).

Materials and methods

Experimental material

Seeds of rice (*Oryza sativa*, *cv.* IR42) and wheat (*Triticum aestivum*, *cv.* Jackson) were imbibed in aerated 0.5 mM $CaSO_4$ for 3–4 h and germinated in Petri dishes on tissue paper moistened with 0.5 mM $CaSO_4$. The Petri dishes were wrapped in aluminium foil, and seeds germinated in a constant temperature room at 30 °C for 3 days. Germinated seeds were then transferred to mesh floats on 50% strength nutrient solution (Colmer et al. 2019) and grown in aerated conditions for 7 days. The nutrient solution was aerated with atmospheric air at 40 ml min^{-1} and light was supplied (PHILIPS MASTER, HPI-T, 400 W/645) at 800 µmol photons m^{-2} s^{-1} (16/8 h light/dark). 10-day-old plants were then transferred to full strength aerated nutrient solution and changed and grown to an age of 28 days from germination at which treatments commenced. The treatment of rice was either (*i*) aerated simulating drained soils, (*ii*) stagnant, deoxygenated simulating soil flooding (Wiengweera et al. 1997) or (*iii*) containing 10% of polyethylene glycol (PEG) 6000 simulating dry soil (resulting in a soil water potential of -0.14 MPa) (see Table 1). PEG-6000 can be used to simulate the low water soil potential with only limited interference with the metabolic processes of the plant (Agrawal et al. 2016). Moreover, 10% PEG was used to simulate a mild osmotic stress considering the moderate tolerance of the IR42 cultivar towards drought (Ponnamperuma 1979). The plants remained under treatments for a week (age 35 days) until new adventitious roots of 100–140 mm length had developed. Wheat plants remained in aerated nutrient solution, and in addition to adventitious roots of 100–140 mm length, we also sampled thin lateral roots of up to 60 mm.

Agar cylinders were used to mimic water loss from artificial roots without any internal tissue structures (i.e. internal barriers to water loss or gas spaces) (Table 1). Agar cylinders of four dimensions (0.8, 1.25, 1.45 and 3.33 mm in diameters) using 3% (w/v) agar solution and 0.03 mM methylene blue (to enhance contrast during time-lapse video recording). The cylinders were prepared using needles or PVC tubes of different sizes (0.8 mm, 1.25 mm, 1.45 mm and 3.33 mm), and the cylinders were stored in

Table 1 Summary of experimental material. Rice or wheat were grown in different types of nutrient solutions to simulate extremes of soil water content. Roots growing in the various conditions formed either formed a weak or a tight barrier to radial O_2 loss (ROL). Agar cylinders with zero porosity were used to isolate the effect of root diameter on radial water loss

Material	Treatment	Simulation	Barrier strength[1]	Root dimension	Resistance factor (α, see Eq. 3)
Rice	Aerated nutrient solution	Drained soil	Weak barrier	Thick adventitious root	$\alpha = 2.03 \times 10^3$
	Stagnant, deoxygenated nutrient solution	Soil flooding	Tight barrier	Thick adventitious root	$\alpha = 10.50 \times 10^3$
	10% polyethylene glycol (PEG-6000) nutrient solution	Dry soil	Tight barrier	Thick adventitious root	$\alpha = 12.75 \times 10^3$
Wheat	Aerated nutrient solution	Drained soil	Weak barrier	Thick adventitious root	$\alpha = 2.10 \times 10^3$
	Aerated nutrient solution	Drained soil	Weak barrier	Thin lateral root	$\alpha = 3.23 \times 10^3$
Agar cylinder	-	0 porosity, solid root	No barrier, no gas space, and no stele	$\varnothing = 0.8, 1.25, 1.45, 3.33$ mm	$\alpha = 1.50 \times 10^3$

[1] For characterization of barrier strength, we used the terminology of Colmer (2003)

deionized (DI) water and cut to the desired length prior to measurements.

Radial water loss

Radial water loss (RWL) was measured by using a gravimetric approach as described by (Peralta Ogorek et al. 2021) with some modifications. Briefly, root segments were positioned on a metallic mesh in a balance chamber with a relative humidity (RH) of 18–28% (HOBO UX100-011 Temperature and RH data logger, Onset). About 150–200 mg fresh mass (FM) of root segments (or agar cylinders) were prepared from intact roots by removing lateral roots and the most apical 30 mm known to rarely develop a ROL barrier (Ejiri et al. 2021). The diameter of the root segments was measured using a digital calliper and the cut ends of roots were sealed with Vaseline. The loss in mass during desiccation was recorded automatically every 30 s for 1 h by using a 5-digit analytical balance (Mettler Toledo Analytical Balance ME54) connected with the software BalanceLink V4.1.3. Meanwhile, the root diameter was monitored by time-lapse images using a USB camera (Dino-Eye Eyepiece Camera) connected with the software Dino-Capture 2.0. The desiccation measurements were taken at 22–24 °C.

Cumulated water loss (% of total water content) and radial water loss (RWL) ($\mu mol\ H_2O\ m^{-2}\ s^{-1}$) were calculated based on total tissue water content and root surface area, respectively. Data of cumulated water loss and RWL were fitted by using a two-phase decay function, with the exception of rice grown in simulated soil flooding or dry soil, where a 6th order polynomial curve showed the best fit. The fitting of data was conducted in order to identify the time for which 15% of total pool of water had been lost (Fig. S1) representing the volume of water present in cells exteriorly to the ROL barrier in rice (Peralta Ogorek et al. 2021). The same procedure was applied to agar cylinders.

To further understand the effect of root size on dynamics of RWL, cross-sections of fresh and dry root segments were prepared. Cross-sections were vertically fixed using clamps and visualized using a stereomicroscope (Olympus, BX60, Olympus Optional CO., LTD Tokyo, Japan) and root circularity (Dudzińska and Piórkowski 2020; Yonis et al. 2020) was determined using ImageJ (see below).

Apoplastic barriers and root cross-sections

A qualitative assay was used to visualize the permeability of the apoplastic barrier following the method described in Soukup et al. (2007) with some modification. Briefly, root segments (25 mm length) were prepared by removing the apical 30 mm and the cut ends were sealed with lanolin. Root segments were incubated in 0.1% (w/v) periodic acid for 1 h, further incubated in a reducing solution (1 g of potassium iodide and 1 g of sodium thiosulfate dissolved in 50 ml of DI water and acidified with 1 ml of 1 M hydrochloric acid)

for 1 h at room temperature. After storing in DI water overnight at 4 °C, the segments were embedded in 5% (w/v) agar for up to 3 days and ca. 100 μm thick cross-sections were prepared using a vibrating microtome (Leica VT1200S, Leica Biosystems). Cross-sections were stained with Schiff's reagent for 3–5 min and periodic acid penetration was visualized under white light in a regular microscope (Olympus, BX60, Olympus Optional CO., LTD Tokyo, Japan). These cross-sections were also used to determine the cortex to stele ratio (CSR).

Methylene blue staining

The qualitative assay of ROL was conducted using methylene blue staining as described by Yamauchi et al. (2019). Methylene blue is a colourless redox indicator in its reduced form and turns blue when oxidized. Plants were trimmed off their leaves (only the leaf sheaths remained) and all of the roots except two target roots 100–140 mm in length. The shoot base with the selected roots was immersed 20 mm below the surface of the solution in a photo chamber containing the reduced methylene blue. The staining pattern of methylene blue on the roots were taken photographs at 1.5 h after the start of the staining experiment.

Root porosity

Root porosity was measured using the pycnometer method as described by (Jensen et al. 1969) with some modification. A 25 ml pycnometer was filled with DI water and weighed (P) using a 5-digit balance (Mettler Toledo Analytical Balance ME54). About 70–120 mg of fresh root tissue, with the 30 mm root tip removed, was weighed (R) and placed into the pycnometer and filled with DI water (Rb+P). Root segments were ground using a mortar, and again transferred to the pycnometer filled with DI water and weighed (Ra+P). The porosity of the roots was then calculated as follows:

$$Porosity(\%) = \left(R_a - R_b \right) / \left(R - R_b \right) \cdot 100 \tag{1}$$

Statistical analyses and image processing

GraphPad Prism software (v.8.3.1) was used for statistical analyses. Differences between treatments were evaluated by using one-way ANOVA followed by Tukey's pairwise test. All data satisfied the assumption of normality (Shapiro–Wilk's test) and homoscedasticity (Bartlett's test) without requiring data transformation.

Photos of fresh and dry root cross-sections were processed using Image J software. Circularity was assessed in order to evaluate the changes in shape due to root desiccation, and calculation was performed using the BioVoxxel plugin for ImageJ (Dudzińska and Piórkowski 2020; Yonis et al. 2020). The circularity was calculated as follows:

$$Circularity = 4\pi \cdot A/P^2 \tag{2}$$

where A is the area of the fresh or dry root cross-sections and P is the perimeter of the fresh or dry root cross-sections.

Numerical modelling

To complement the experimental investigation, we developed a simplified numerical model to predict the behaviour with time of cumulated water loss and RWL in roots and agar cylinders. The model is based on the assumption that water (in the form of water vapour) leaves the root by diffusion and, due to this loss of water, the root shrinks.

Therefore, starting from the mass balance equation, we first calculated the diffusion of water vapour out of the root (assumed to be perfectly cylindrical), solving the diffusion equation of cylindrical coordinates (Truskey et al. 2010):

$$\frac{\partial C}{\partial t} = \frac{1}{r} \frac{\partial}{\partial r} \left(rD \frac{\partial C}{\partial r} \right) \tag{3.1}$$

where C is the concentration of water vapour in air, r is the radial coordinate and D is the diffusion coefficient. The concentration at the surface of the root (location r_i) is assumed to be equal to the concentration inside the root, C $(r=r_i)=C_i$. In this case, at the beginning of the process $C_i=(1-\Phi)\cdot55.5\times10^3$ mol/m^3 (liquid water homogenously distributed inside the root volume), with Φ the apparent solid fraction of the root that cannot be occupied by water (solid material and pores not accessible to water). Moreover, the concentration far from the root surface (at radius $r_e=10^3 r_i$) is equal to the concentration of water vapour in air at the given humidity (18–28% RH). By solving Eq. 3.1, we obtain the behaviour of the

concentration in time and space in the ambient air surrounding the root, $C(r, t)$.

Then, the RWL can be obtained from Fick's 1st law of diffusion (Fick 1855) as

$$RWL = -D_s \left[\frac{\partial C}{\partial r} \right]_{r_i} \tag{3.2}$$

where Ds is an equivalent diffusion coefficient at the root surface. Note that Ds takes into account the complex physics that happens inside the root and at the root surface, like capillary trapping of water drops, surface permeability and/or the presence of resistances to the flow (endodermis, exodermis and apoplastic barriers), and can be expressed as

$$D_s = D / \alpha \cdot \sqrt{r_i} \tag{3.3}$$

where α is a resistance factor introduced to simulate the presence of the barrier to ROL. In order to simulate the resistance of the endodermis of wheat roots (a structure absent in the agar cylinders) or the exodermis (and sclerenchyma) present in rice roots, α was set at a value > 1 (Tables 1 and 2). The expression of D_s represents a combination between a constant and uniform diffusion coefficient (which is the simplest assumption usually employed to simulate diffusion processes through homogenous media) and a diffusion coefficient that varies linearly with r_i (typical of surface tension phenomena that occur at the interface between two different phases), and mimics reasonably well the current situation of mass transport through a root surface.

The cumulated water loss, W, can be obtained:

$$W(t) = \int_0^t RWL(\tau) \cdot S(\tau) d\tau \tag{3.4}$$

where $S(\tau)$ the value of the external surface of the root at the given time instant. As water leaves the root, the root loses mass and shrinks. From the mass balance of water contained inside the root, we get:

$$\frac{dr_i(t)}{dt} = -\frac{RWL(t)}{C_i} \tag{3.5}$$

Note that there is a minimum radius, $r_{i,min} = \Phi^{(1/2)} \cdot r_i(0)$, which corresponds to the situation in which the inner root structure (composed by solid fibres and non-accessible pores) is fully packed. When the root radius reaches this minimum value, the root cannot shrink further. Due to the loss in mass, and to the corresponding shrinkage effect, the mass of water inside the root changes, and so does the volume of the root. As a consequence, at each time step, we recomputed the concentration of water inside the root as follows:

$$C_i = \frac{W_0 - W(t)}{\pi r_i(t)^2 LM\Phi} \tag{3.6}$$

where W_0 is the water present inside the root at the beginning of the process (time $t=0$), L is the length of the root (we assume $L=1$ in the computations), and M is the molar mass. This concentration is then used as a boundary condition to solve Eq. 3.1, and to start the loop again.

Table 2 Modelling scenarios from 1 to 10 showing simulated root diameter, tissue porosity, solid fraction and barrier to radial O₂ loss (ROL). Symbols - and + mean absence or presence of the barrier to ROL, respectively

Case	Root diameter (mm)	Porosity (%)	Solid fraction[1]	ROL barrier	Resistance factor (α, see Eq. 3)
1	0.5	3	0.03	-	$\alpha = 1.50 \times 10^3$
2	1.0	3	0.03	-	$\alpha = 1.50 \times 10^3$
3	2.0	3	0.03	-	$\alpha = 1.50 \times 10^3$
4	4.0	3	0.03	-	$\alpha = 1.50 \times 10^3$
5	1.0	10	0.15	-	$\alpha = 1.50 \times 10^3$
6	1.0	30	0.45	-	$\alpha = 1.50 \times 10^3$
7	0.5	3	0.03	+	$\alpha = 12.75 \times 10^3$
8	1.0	3	0.03	+	$\alpha = 12.75 \times 10^3$
9	1.0	10	0.15	+	$\alpha = 12.75 \times 10^3$
10	1.0	30	0.45	+	$\alpha = 12.75 \times 10^3$

[1] for explanation of the *solid fraction* parameter, please see materials and methods

Results

Functional changes in the root exodermis

Growth conditions simulating soil flooding or dry soil both induced a barrier to radial oxygen loss (ROL) as well as an apoplastic barrier (Fig. 1). Formation of a barrier to ROL was evaluated by methylene blue, which is a colourless redox indicator in its reduced form and turns blue when oxidized. Therefore, a blue halo forming around the roots is showing that oxygen diffuses radially from the root to the solution. In stark contrast, roots of rice grown in aerated solution (simulating drained soil) only developed a weak barrier, as indicated by the blue staining along the entire root axis (Fig. 1A). Our results show convincing evidence for ROL barrier formation in roots of rice both when grown in stagnant deoxygenated solution (simulating soil flooding) but also in treatments with PEG-6000 (simulating dry soil). Staining was absent at the main axis of these roots indicating that a tight ROL barrier had formed (Fig. 1B, C). Meanwhile, a blue halo

formed at the root apices (Fig. 1B, C) where the ROL barrier is rarely induced (Shiono et al. 2011). Importantly, the blue halo at the root tip indicates that the absence of staining at the mature root zones is indeed due to a ROL barrier rather than low tissue O_2 status; the latter can happen if the cortex is very low in porosity, if the aerenchyma becomes flooded or otherwise damaged (Pedersen et al. 2021a). Thick adventitious roots of wheat as well as thin lateral roots of wheat stained blue at the basal part of the root, indicating some loss of oxygen and therefore the presence of only a weak barrier to ROL (Colmer 2003) (Fig. S6A, B).

The ROL barrier has been suggested to result from suberization and/or lignification of the cell walls in the root exodermis forming an apoplastic barrier (Kotula et al. 2009b). The presence or absence of such a barrier was visualized using periodic acid staining. The roots of rice with a tight barrier to ROL had also formed an apoplastic barrier indicated by only the outer cell layers of cross-sections being stained purple (Fig. 1E, F). In contrast, the cortex
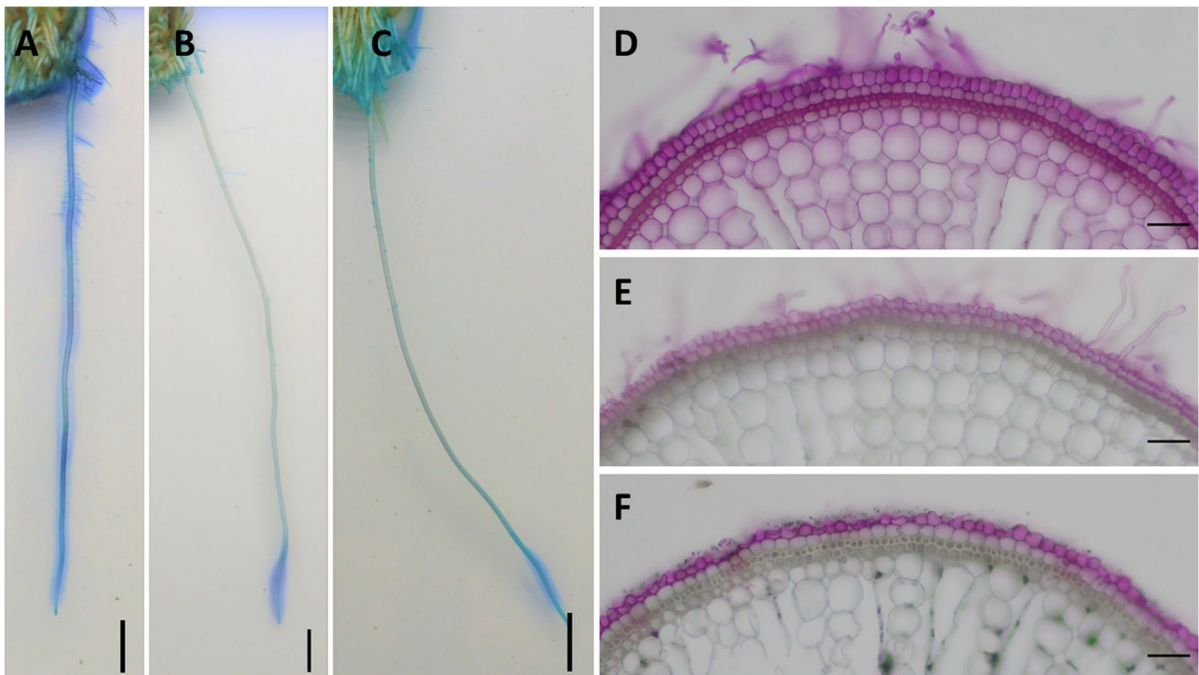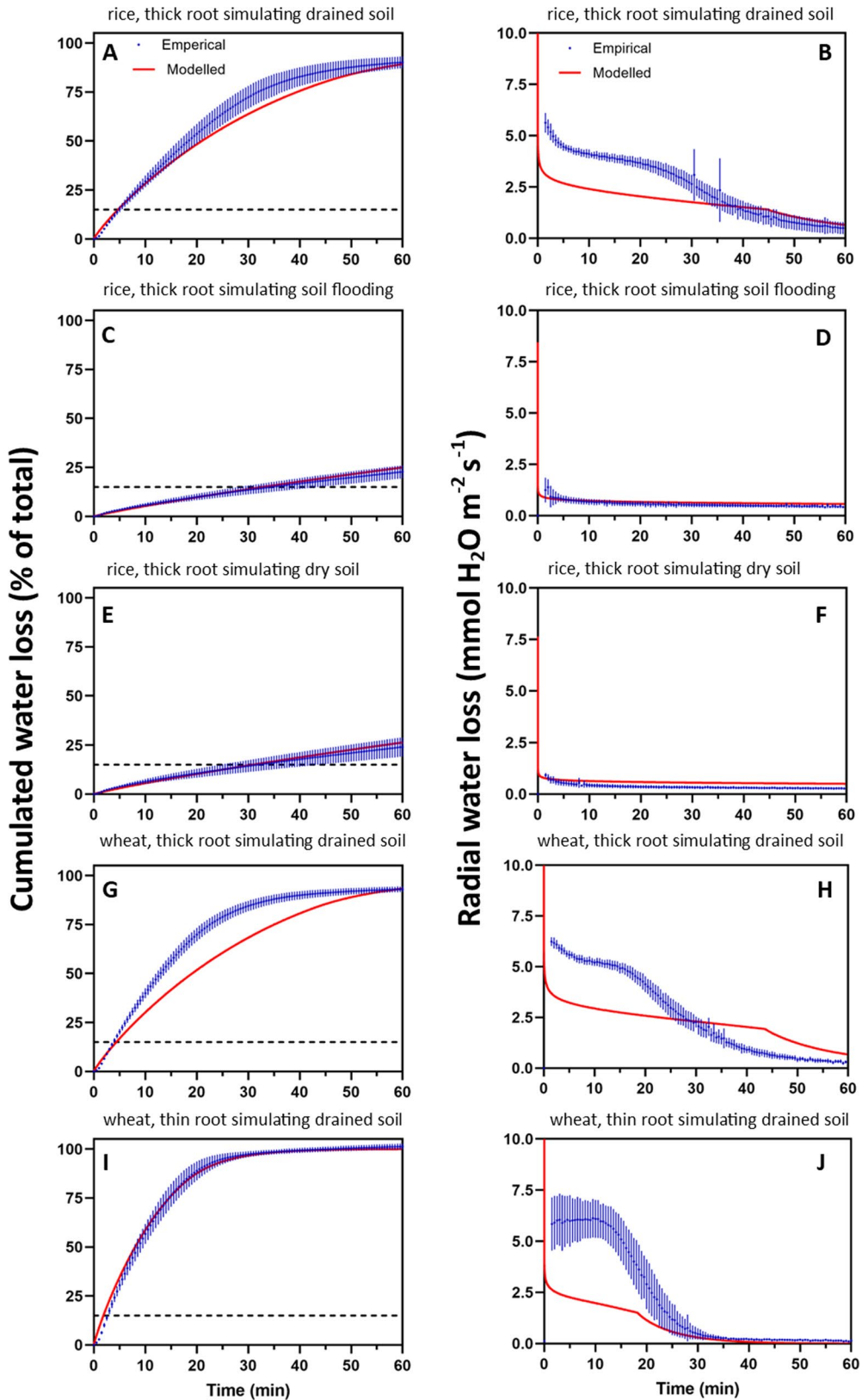

Fig. 1 Methylene blue (**A**-**C**) and periodic acid staining (**D**-**F**) of rice roots. In A-C, blue coloration indicates radial O_2 loss (ROL) and in D-F, purple coloration indicates radial infiltration of the apoplastic tracer. Plants were 28- to 35-day-old and in A, D, plants were grown in aerated nutrient solution (simu-lating drained soil), in B, E, stagnant, deoxygenated nutrient solution (simulating soil flooding) and in C, F, in nutrient solution with PEG-6000 (simulating dry soil). Scale bar = 1 cm in A-C and 50 µm in D-F

rice, thick root simulating drained soil

rice, thick root simulating soil flooding

rice, thick root simulating dry soil

wheat, thick root simulating drained soil

wheat, thin root simulating drained soil

of root cross-sections in rice with a weak barrier as well as the two types of wheat roots stained purple throughout the cortex indicating that they had not formed a tight apoplastic barrier (Fig. 1D, S6C and D). Our results therefore show that roots of rice can form a barrier to ROL and an apoplastic barrier as a response to soil flooding as well as to low soil water content.

Effects of key root traits on radial water loss

Root segments of rice and wheat desiccated when exposed to a dry atmosphere, but key root traits substantially influenced the rate of desiccation. The root ROL barrier significantly restricted rates of both cumulated water loss and radial water loss (RWL) (Fig. 2A-F). This is evidenced by empirical data showing that roots with a tight barrier only lost 15% of their initial water content after 30 min of exposure to dry air (Fig. 2C, E), and only 20–25% after 60 min (Fig. 2C, E). In stark contrast, roots of rice with a weak barrier (Fig. 1A) had lost 15% of total water content already after 5 min (Fig. 2A). Furthermore after an initial decline, RWL levelled out after 10 min in roots of rice with a tight barrier (Fig. 2D, F), whereas rates of RWL continued to decline for 55 min in roots with a weak barrier (Fig. 2B).

In roots forming an exodermis (e.g., rice), the amount of root tissue positioned exteriorly to the exodermis is approximately 15% (Peralta Ogorek et al. 2021). Moreover, rates of RWL are driven by difference in water potential between the tissue and the surrounding air and therefore comparisons between different types of roots need standardization. Assuming that the tissue desiccation takes place from the surface and inwards, we used 15% of total water loss

to compare the rates of RWL in rice grown in three different conditions with that in wheat grown in aerated solution. The comparison showed that RWL in rice were 9 to 13-fold higher in roots with a weak barrier (drained soil) compared to roots with a tight barrier (soil flooding or dry soil) (Fig. 3A). Furthermore, thin roots of wheat had the highest rates of RWL, and thick roots of wheat had a much higher RWL than that of rice roots with a weak barrier showing that the exodermis in itself (absent in wheat) presents some resistance to desiccation (Fig. 3A).

As hypothesized, rates of cumulated water loss and RWL were also strongly affected by root thickness, i.e. thick roots showed lower rates of water loss compared to thin roots (Fig. 2G-J). Including roots of wheat in this study enabled us to assess the influence of root thickness without the confounding effect of an exodermis and, moreover, wheat never form a tight barrier to ROL (Garthwaite et al. 2006). The absence of tight ROL barrier in wheat was evident from the rates of cumulated water loss as thick roots (0.7–0.9 mm) had lost 15% after 4 min and 90% after 40 min (Fig. 2G). In thick roots, rates of RWL were below detection limit after 50 min (Fig. 2H), indicating almost complete desiccation of the roots. In thin roots (0.2–0.3 mm), water loss was even faster as the cumulated water loss had reached 15% already after 3 min and approached 100% after 30 min. (Fig. 2I). It is interesting to note that the RWL curve shows a two-phase behaviour (see for example Fig. 2B-H-J), characterized by an initial rapid decrease, which slowly levels off, followed by a second sharper decrease. The inception of the second stage (the kink in the RWL curve) occurs when the root has reached its minimum diameter, i.e. when it cannot shrink further because of structural constraints. This behaviour is also nicely captured by the numerical model.

In order to isolate the effect of root diameter, we used artificial roots made from agar as these have zero "tissue porosity", are lacking a stele, an exodermis and a ROL barrier. Rates of cumulated water loss and RWL from agar cylinders were controlled by the diameter of these cylinders (Fig. S1). Cylinders of 0.8 mm in diameter reached 100% of cumulated water loss, and therefore also rates of RWL below detection limit, after 50 min (Fig. S1A, B). By contrast, 1.25, 1.45 and 3.33 mm cylinders only lost 70, 72 and 30% of total water content after 60 min, respectively (Fig. S1C, E, G). Rates of RWL at the time point at

Fig. 3 A, radial water loss (RWL) at the time at which 15% ▶
cumulated water loss had occurred (see Fig. 2A, C, E, G and
I). **B**, cortex to stele ratio (CSR) with bars representing the
mean and error bars (standard deviation). **C**, tissue porosity
expressed as percentage gas spaces per volume of tissue. Plants
were grown in aerated nutrient solution (simulating drained
soil), stagnant, deoxygenated nutrient solution (simulating soil
flooding) and with PEG-6000 nutrient solution (simulating dry
soil). In box-whisker plots (A and C), the boxes represent 50%
quartiles, whiskers minimum and maximum of values and the
horizontal line the median. Different letters indicate significant
difference ($P < 0.01$, Tukey's test, $n = 5$). *n.a.,* data not available

which 15% of total water content had evaporated in
1.25, 1.45 and 3.33 mm cylinders were 25, 19 and
57% lower than that of the 0.8 mm cylinder, respec-
tively (Fig. S1D, F, H). These results underline that
while rates of cumulated water loss and RWL are
profoundly affected by the barrier to ROL, water loss
also depends strongly on root thickness.

In an effort to single out the effect of three key root
traits on cumulated water loss and RWL, we com-
plement our experimental results with correspond-
ing predictions obtained from the numerical model
described above. The main parameters of the model
were root diameter, tissue porosity and the presence/
absence of a barrier to ROL. Other physical resist-
ances to the flow of water (i.e. presence/absence of
exodermis and of endodermis) are also captured by
the parameter α, which lumps together all the phys-
ics occurring within the root and at the root surface
(see Tables 1 and 2). In most cases, predicted cumu-
lated water loss as well as RWL were in close agree-
ment with the obtained experimental data (Fig. 2A,
C-F, I). However, there were also cases characterized
by a slightly larger deviation between the measured
(experimental) and predicted (numerical) desicca-
tion pattern (Fig. 2B, H, J). For the agar cylinders,
the experimental and predicted values were also in
nice agreement, but for the RWL of the thin agar cyl-
inders, the model was unable to reflect the dramatic
changes in RWL during time (Fig. S1A-S1B). The
increase in RWL of the thin cylinders were caused by
a rapid decline in surface area (Fig. S4), and possi-
bly by a corresponding complex cross sectional shape
(low circularity) that is not taken into account in the
model (which assumes a perfectly circular, symmetri-
cal shape).

In addition to the direct influence on water loss,
the growth conditions also influenced some other root
traits. The CSR of rice roots responded significantly
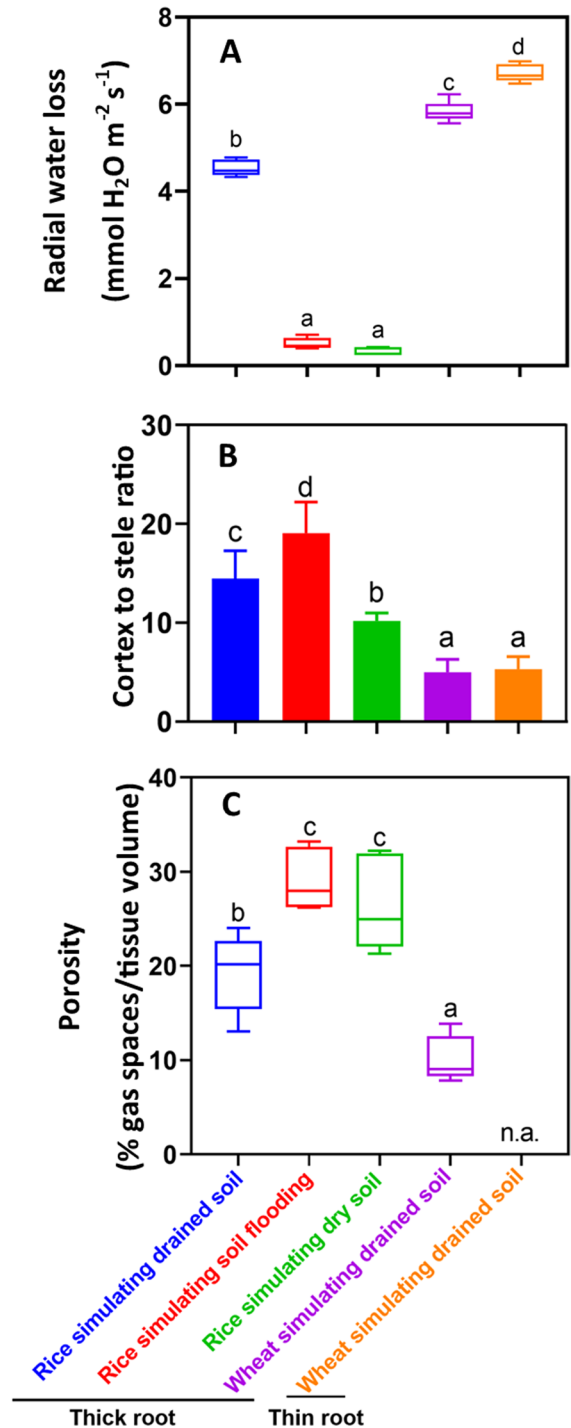
to treatments (Fig. 3B). Compared to aerated condi-
tions (drained soils), CSR increased by 23% in stag-
nant, deoxygenated conditions (soil flooding) but was
reduced by 28% in treatments with PEG-6000 (dry

Fig. 4 Dynamics of changes in root shape of rice and wheat ▶ during exposure to dry air (relative humidity 18–28%). In **A**, **B**, time-lapse images of root segments of rice grown in aerated nutrient solution; in **C**, **D**, time-lapse images of root segments of rice grown in stagnant, deoxygenated nutrient solution. In **E**, changes in root diameter with time in root segments of rice and in **F**, changes in root diameter with time in thick or thin root segments of wheat. Symbols represent the mean $\pm$ SD ($n=5$). In **G**, changes in circularity (based on root cross-sections at the beginning (t_0) and the end (t_{60}) of 60 min of exposure to dry air in root segments of rice and wheat. Plants were grown in aerated nutrient solution (simulating drained soil), stagnant, deoxygenated nutrient solution (simulating soil flooding) and with PEG-6000 nutrient solution (simulating dry soil). Bars are means $\pm$ SD ($n=5$); ****, $P < 0.0001$; n.s., no significance for two-tailed Student's t-test. *n.a.,* data not available

soils). In comparison, CSR did not differ significantly between thick and thin roots of wheat. Root porosity also responded to growth conditions (Fig. 3C). Root porosity of rice roots was 34 and 28% higher in roots formed in stagnant, deoxygenated solution or in PEG-6000, respectively, than in rice roots formed in aerated solution. These results show that other key anatomical root traits in rice respond similarly to soil flooding or conditions of low soil water potential.

Dynamics of changes in root shape during desiccation

Time-lapse video recordings of roots during desiccation revealed significant differences in responses to desiccation. The most reduced striking effect was that of roots with the ROL barrier, which effectively maintained root circularity during the 1 h of desiccation (Fig. 4G, S5). In roots grown in stagnant, deoxygenated solution (soil flooding) as well as in PEG-6000 (dry soil), the diameter and the circularity were unaffected by tissue water loss (Fig. 4E, G). In contrast, in roots of rice grown in aerated solution (drained soil), the root diameter decreased by 42% within 1 h, a response also seen in roots of wheat although more pronounced (thick wheat roots had declined by 62% already after 35 min and the thin wheat roots by 54% within 10 min) (Fig. 4E, F). As the roots were shrinking during desiccation, the shape also changed significantly from a circular shape to a polygon (Fig. 4F, G and S5). The agar cylinders supported the observations from roots showing that the thin cylinders changed significantly more
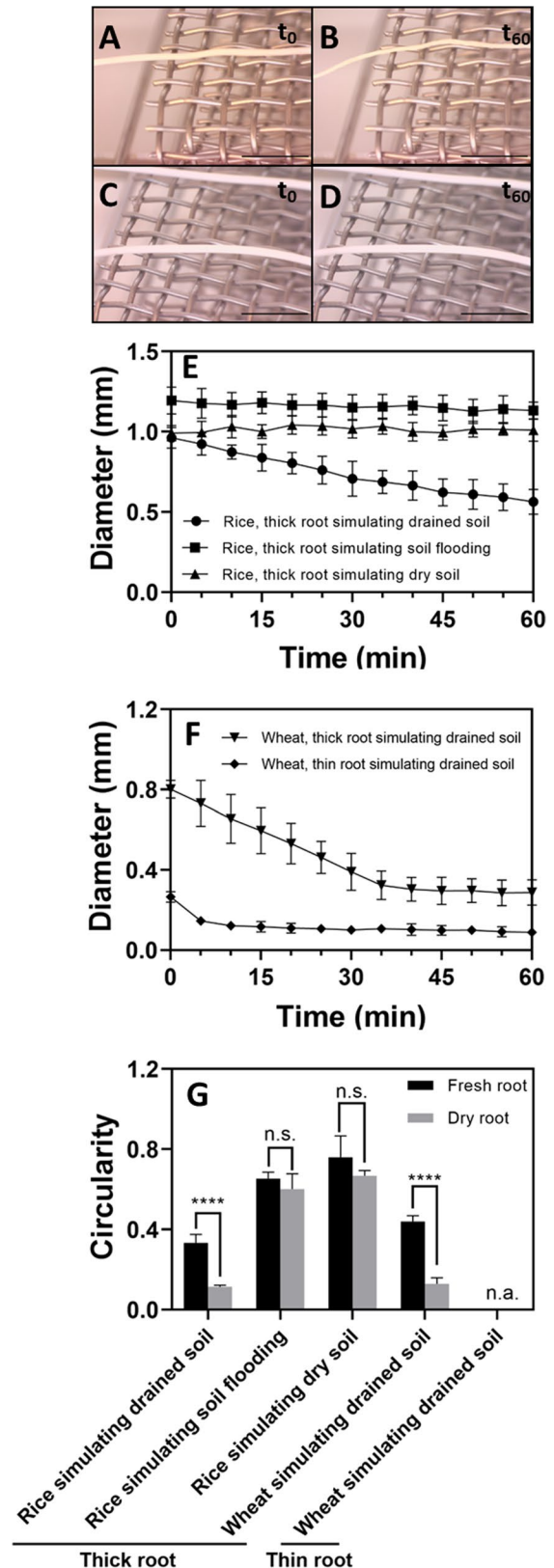
in diameter during the course of desiccation compared to the thicker ones (Fig. S4).

The faster desiccation of thin cylinders were due to profound differences in SA:V driving water loss. RWL followed a linear relationship with changes in SA:V, i.e. higher SA:V (thin cylinders) showed higher rates of radial water loss (Fig. S3). Importantly, treatments inducing a barrier to ROL in rice (i.e. soil flooding and dry soil) can be recognized as outliers since the barrier shows much stronger effect on desiccation than the SA:V (Fig. S3). Radial water loss of the thin wheat roots also followed a pattern different to that of the agar cylinders showing lower RWL than predicted by the SA:V (Fig. S3).

Discussion

Root traits are known to respond to soil water availability (Knutzen et al. 2015), and some of them can affect radial water loss (RWL) when roots grow in dry soils. Therefore, an important aim of the present study was to assess the quantitative importance of key root traits for RWL using a mathematical model. The model was benchmarked against experimental data from roots of rice and wheat. We found that low water availability induced a barrier to radial oxygen loss (ROL) in roots of rice and the barrier significantly restricted RWL. Furthermore, the surface area to volume ratio (SA:V) of roots was positively correlated to RWL, i.e. thin roots lost water faster than thick roots. Below, we discuss these findings with focus on the formation of the barrier and how key root traits (the barrier, tissue porosity, diameter, and SA:V) affect RWL based on experimental data as well as predicted data from our model.

Low water potential induces a tight barrier to radial oxygen loss in roots of rice

The barrier to ROL is a "jack of all trades" serving multiple roles in protecting roots from different abiotic stressors (Pedersen et al. 2021b; Peralta Ogorek et al. 2021; Yamauchi et al. 2021a). The ROL barrier is formed under stagnant, deoxygenated conditions (soil flooding) but high CO_2, low oxygen or exogenous ethylene did not induce a barrier formation (Colmer et al. 2006). Instead, reduced Fe (Mongon et al. 2014) and low molecular carboxylic

acids (Colmer et al. 2019) acted as environmental signals for ROL barrier formation, and H_2S further strengthened a ROL barrier already formed in stagnant, deoxygenated nutrient solution (Armstrong and Armstrong 2005). These environmental signals are all produced by microbes in flooded, anoxic soils, where the resulting ROL barrier restricts oxygen loss and facilitates oxygen supply to the growing root tip (Sanderson and Armstrong 1980), and in some cases also restricts intrusion of soil phytotoxins (Jimenez et al. 2021). In the present study, we found that ROL was greatly restricted from the basal parts of the roots regardless of the roots were formed in stagnant, deoxygenated solution or in PEG-6000 (Fig. 1B, C). This observation shows that a tight ROL barrier had formed in both conditions, as radial oxygen diffusion was restricted to the root apex. It is indeed a novel finding that low water potential in the nutrient solution can also act as a signal for ROL barrier formation suggesting additional roles of the barrier.

One such role has recently been demonstrated in roots of rice, where a tight ROL barrier formed in stagnant, deoxygenated nutrient solution significantly restricted RWL (Peralta Ogorek et al. 2021). In the present study, roots grown in PEG-6000 (dry soil) or in stagnant, deoxygenated nutrient solution (soil flooding) both showed significantly lower rates of RWL compared to control plants grown in aerated nutrient solution (drained soil) (Fig. 3A). The strength of the barrier formed as a response to the two growth conditions does not differ significantly when based on rates of RWL (Fig. 3A) or ROL (Fig. 1B, C). However, staining by the apoplastic tracer (periodic acid) suggests some histochemical differences. The apoplastic barrier formed in stagnant, deoxygenated conditions was positioned 1–2 cell layers further into the root as compared to the barrier formed in PEG-6000, where only the epidermis stained purple (Fig. 1E, F). This indicated that the apoplastic barrier was already present in the cell layer immediately below the epidermis when formed in PEG-6000. It was beyond the scope of the present study to identify the active components of the apoplastic barrier, and currently both lignin and suberin are candidate components of the ROL barrier with most studies suggesting that suberin is more important in determining barrier strength (Kulichikhin et al. 2014; Schreiber et al. 2005; Soukup et al. 2007). We propose that the apoplastic barrier in the root exodermis could indeed

be formed by different cell wall components depending on the environmental signals.

Response of key anatomical root traits to growth conditions

Inducible aerenchyma is known to form as a response to soil flooding (Yamauchi et al. 2019) as well as to low soil water potential (Lynch et al. 2014). In both cases, programmed cell death leads to large gas-filled volumes in the root cortex, but the function differs in the two environmental situations. During soil flooding, the aerenchyma forms a low-resistance diffusion pathway to supply oxygen to the growing root tips (Sanderson and Armstrong 1980), whereas the aerenchyma in dry soils serves to conserve water and resources, i.e. longer roots can be formed for the same investment in water and organic carbon (Lynch 2018; Yamauchi et al. 2021b). However, aerenchyma can impede radial water uptake via the cell-to-cell pathway due to the gas spaces where radial water uptake can only occur through the apoplastic pathway (Ouyang et al. 2020; Yang et al. 2012). In present study, we measured tissue porosity, which in addition to aerenchyma also includes small intercellular, gas-filled spaces. We also found that porosity was significantly enhanced by both stagnant, deoxygenated conditions and by PEG-6000 and tissue porosity did not differ between the two situations (Fig. 3C). Interestingly, tissue porosity increased RWL showing that aerenchyma formation as a response to low soil water potential comes at a cost (see modelling below, Fig. 5B). It is well known that key root traits vary substantially with tissue age. Aerenchyma is more pronounced at the basal part of a root compared the apical part (Yamauchi et al. 2013). Therefore, RWL might not be significantly affected by porosity in young root tissues (apical parts) but, similarly to ROL, the RWL would be influenced by the immature exodermis (Ranathunge et al. 2004; Yamauchi et al. 2019), which do not form a barrier to ROL, and also by the smaller diameter of the root in proximity to the tip. In contrast, RWL would be substantially restricted at the root base due to the larger root diameter (smaller SA:V) and the well-developed exodermis (and sclerenchyma) (Kotula et al. 2009a; Yamauchi et al. 2019).

Another key root trait known to respond to water availability, either too much or too little, is the cortex to stele ratio (CSR) (Yamauchi et al. 2019). In the present study, the CSR was significantly higher in stagnant, deoxygenated conditions deriving from a larger cortex containing 12–13 cells in each file, whereas the lower CSR in PEG-6000 was due to a lower number of cells (9–10) in each file as well as a larger stele (data not shown). Compared to rice roots grown in aerated condition, CSR in rice roots grown in stagnant, deoxygenated condition was significantly enhanced while it was decreased in rice roots grown in PEG-6000 solution (Fig. 3B). The results of CSR responding to deoxygenated, stagnant and low water potential growth conditions confirmed a previous study by Yamauchi et al. (2021b) who found that CSR increased with the increasing of soil water content in 18 wild Poaceae species. For drought conditions, the increase of the stele area allows more water transport in xylem vessels, which can promote the growth of shoots (Henry et al. 2012). For flooded conditions, the increase of cortex area shows that roots can accommodate more formation of aerenchyma which is beneficial for gas transport from the basal root zone to apices (Yamauchi et al. 2021a). Therefore, the apparent contrasting result showing the decrease in CSR concomitant with an increase in root porosity in rice is not surprising. Smaller CSR (driven by a larger stele) ameliorates water uptake and or transport, whereas the increase in root porosity reduces the metabolic cost for root elongation, which can be demanding for plants growing in dry soils with a deep water table (Yamauchi et al. 2021b).

Interestingly, the formation of a barrier to ROL indirectly influences an important root trait, i.e. the circularity of the root. We found no significant difference in circularity between fresh, fully hydrated roots and desiccated roots when a barrier to ROL had been induced, and the benefits of a suberized/lignified exodermis was present regardless of the ROL barrier having been formed as a response to soil flooding or low soil water content (Fig. 4G, S5C-F). Suberization or lignification enhances the rigidity of the exodermis preventing a collapse of the cortex, which was otherwise observed in the rice roots without a barrier to ROL as well as in roots of wheat (Fig. S5A, B, G, H). Maintaining circularity (a proxy for root contact with the surrounding rhizosphere) is important as cortex shrinking has been shown to impede water uptake (Carminati et al. 2009). Cortex shrinkage has been observed not only at low soil
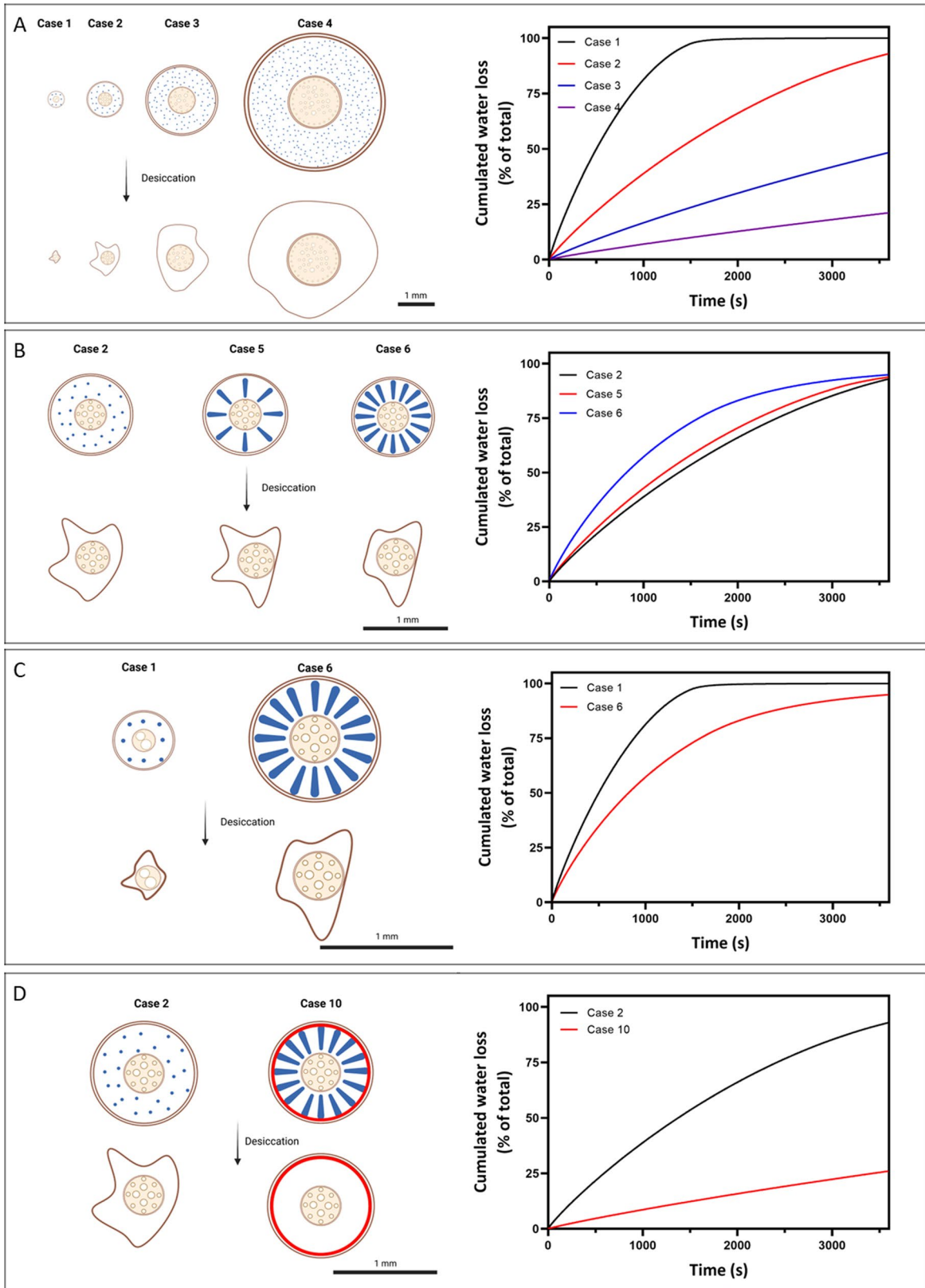
◄**Fig. 5** Predictions of cumulated water loss from roots with contrasting key traits. **A**, shows the effect of root diameter ranging from 0.5 to 4.0 mm in diameter all at low tissue porosity. **B**, shows the effect of tissue porosity between 3%, 10% and 30% all at constant root diameter (1.0 mm). **C**, shows the combined effect of root diameter (0.5 or 1.0 mm) and tissue porosity (3% or 30%). **D**, shows the effect of the barrier to radial oxygen loss with constant root diameter (1 mm). A scenario showing the combined effects of size (0.5 or 4.0 mm) *versus* the barrier to radial oxygen loss (±) is shown in SI Fig. S7

water potential but also as a consequence of extensive transpiration (Carminati et al. 2017), but water uptake can be restored by closing the root-soil gaps (Faiz and Weatherley 1982). We therefore propose that a suberized/lignified exodermis can help maintaining the root-soil contact and thereby sustain nutrient and water uptake during times of low water availability or elevated water demand.

Modelling of the combination of key root traits to radial water loss

We constructed a numerical model to visualize the effect of three key root traits (diameter, tissue porosity and possible presence of a barrier to ROL) on cumulated water loss and rate of RWL. In order to demonstrate the driving forces of root desiccation, we selected a number of contrasting modelling scenarios (Table 2). The significant effect of root diameter is clearly demonstrated in Fig. 5A showing that thin roots are considerably more prone to desiccation than thick roots (for clarity, only cumulated water loss is shown, Table 2 scenarios 1 to 4) and the faster desiccation is driven by a higher SA:V in thin roots compared to thick roots (Fig. S3). Similarly, the amount of aerenchyma also affects root desiccation, i.e. the more aerenchyma, the faster the tissue desiccation (Fig. 5B). If there are more gas-filled tissues, there is also less water per volume of root and therefore the desiccation is faster since there is less water to be lost before it becomes critical to root function. The adverse impact of a small diameter can be effectively offset by a larger diameter even if it is combined with much higher tissue porosity (Fig. 5C), i.e. the desiccation risk can be counteracted simply by forming a thicker root, and the extra cost in carbon (and water) for the thicker root can be partly compensated by forming aerenchyma. Finally, the significant effect of the ROL barrier is also captured by the model

(Fig. 5D); even if large amounts of aerenchyma would accelerate desiccation, the barrier seems able to restrict radial water loss. However, the ROL barrier effect cannot account for the huge effect of SA:V demonstrated by the scenarios 4 vs. 7 where a 4 mm root without a barrier is compared to a 0.5 mm root with a ROL barrier (Fig. S7). Here, the 8-fold difference in SA:V overrules the protective effect of the ROL barrier.

To conclude, a thick root has greater penetration ability in dry, hard soils as they are more resistant to buckling and deflection (Lynch et al. 2021) and the thick roots lose water at a much slower pace than thin roots. The extra costs of forming thick roots can be reduced by formation of cortical aerenchyma but the aerenchym formation will increase the risk of desiccation. Our data suggested that rice responds to soil water limitations by forming thin roots (Azhiri-Sigari et al. 2000) even if our modelling has demonstrated that this strategy comes with a risk of increasing RWL to the dry topsoil. We did not investigate the role of root hairs on RWL despite their possible function in flood and drought stress responses. Similarly to root apices (Peralta Ogorek et al. 2021), root hairs are likely to act as windows for ROL and RWL. They are quickly formed by the plant and length as well as density can be affected by growing conditions (Nestler et al. 2016), including soil moisture (Haling et al. 2014). Moreover, a study on wild species of Poaceae revealed that species growing at low soil water content (< 25%) have equal or slightly larger root diameter compared to those growing under non-stressful soil moisture conditions (25–45% soil water content) (Yamauchi et al. 2021b), indicating that thinner root may present a risk of desiccation under very low soil water potentials.

Conclusion

Our study showed that low water potential in the nutrient solution of hydroponics resulted in ROL barrier formation in roots of rice as indicated by methylene blue staining. Similarly, an apoplastic barrier, as identified by the apoplastic tracer periodic acid, was also formed. The barrier significantly restricted RWL, but root diameter and tissue porosity also influenced RWL. Importantly, the barrier prevented roots from shrinking during desiccation. Our numerical model

reflected the empirical data and clearly demonstrated that thick roots and a barrier to ROL restricts RWL while cortical porosity accelerates it. Our modelling approach highlighted that increase in root tissue porosity, a common response to drought, conserves water when new roots are formed, but the higher desiccation risk related to high-porosity roots can be effectively counteracted by forming thick roots or even better, by a barrier to ROL.

Author contribution Conceptualization (ZS, FZ, EP, OP), methodology (ZS, FZ, LLOP, EP, OP, MH), investigation (ZS, FZ, VKB), analysis (ZS, FZ, EP, OP), visualization (ZS, FZ, OP) and writing (ZS, FZ, LLOP, VKB, MZ, EP, OP). All authors approved the final version of the manuscript.

Declarations

References

Agrawal L, Gupta S, Mishra SK, Pandey G, Kumar S, Chauhan PS, Chakrabarty D, Nautiyal CS (2016) Elucidation of complex nature of PEG induced drought-stress response in rice root using comparative proteomics approach. Front Plant Sci 7:1466. https://doi.org/10.3389/fpls.2016.01466

Armstrong J, Armstrong W (2005) Rice: sulfide-induced barriers to root radial oxygen loss, Fe^{2+} and water uptake, and lateral root emergence. Ann Bot 96:625–638. https://doi.org/10.1093/aob/mci215

Azhiri-Sigari T, Yamauchi A, Kamoshita A, Wade LJ (2000) Genotypic variation in response of rainfed lowland rice to drought and rewatering: II. Root growth. Plant Prod Sci 3:180–188. https://doi.org/10.1626/pps.3.180

Carminati A, Vetterlein D, Weller U, Vogel H-J, Oswald SE (2009) When roots lose contact. Vadose Zone J 8:805–809. https://doi.org/10.2136/vzj2008.0147

Carminati A, Benard P, Ahmed MA, Zarebanadkouki M (2017) Liquid bridges at the root-soil interface. Plant Soil 417:1–15. https://doi.org/10.1007/s11104-017-3227-8

Colmer TD (2003) Long-distance transport of gases in plants: a perspective on internal aeration and radial oxygen loss from roots. Plant Cell Environ 26:17–36. https://doi.org/10.1046/j.1365-3040.2003.00846.x

Colmer TD, Gibberd MR, Wiengweera A, Tinh TK (1998) The barrier to radial oxygen loss from roots of rice (*Oryza sativa L.*) is induced by growth in stagnant solution. J Exp Bot 49:1431–1436. https://doi.org/10.1093/jexbot/49.325.1431

Colmer TD, Cox MC, Voesenek LA (2006) Root aeration in rice (*Oryza sativa*): evaluation of oxygen, carbon dioxide, and ethylene as possible regulators of root acclimatizations. New Phytol 170:767–777. https://doi.org/10.1111/j.1469-8137.2006.01725.x

Colmer TD, Kotula L, Malik AI, Takahashi H, Konnerup D, Nakazono M, Pedersen O (2019) Rice acclimation to soil flooding: Low concentrations of organic acids can trigger a barrier to radial oxygen loss in roots. Plant Cell Environ 42:2183–2197. https://doi.org/10.1111/pce.13562

Comas LH, Becker SR, Cruz VM, Byrne PF, Dierig DA (2013) Root traits contributing to plant productivity under drought. Front Plant Sci 4:442. https://doi.org/10.3389/fpls.2013.00442

Cruz RT, Jordan WR, Drew MC (1992) Structural changes and associated reduction of hydraulic conductance in roots of *Sorghum bicolor* L. following exposure to water deficit. Plant Physiol 99:203–212. https://doi.org/10.1104/pp.99.1.203

Dhankher OP, Foyer CH (2018) Climate resilient crops for improving global food security and safety. Plant, Cell Environ 41:877–884. https://doi.org/10.1111/pce.13207

Drew MC (1992) Soil aeration and plant root metabolism. Soil Sci 154:259–268

Dudzińska D, Piórkowski A (2020) Tissue differentiation based on classification of morphometric features of nuclei. International Conference on Applied Informatics. Springer

Ejiri M, Fukao T, Miyashita T, Shiono K (2021) A barrier to radial oxygen loss helps the root system cope with waterlogging-induced hypoxia. Breed Sci 71:40–50. https://doi.org/10.1270/jsbbs.20110

Enstone DE, Peterson CA, Ma F (2003) Root endodermis and exodermis: structure, function, and responses to the environment. J Plant Growth Regul 21:335–351. https://doi.org/10.1007/s00344-003-0002-2

Faiz SMA, Weatherley PE (1982) Root contraction in transpiring plants. New Phytol 92:333–343. https://doi.org/10.1111/j.1469-8137.1982.tb03391.x

Fick A (1855) Ueber diffusion. Annalen der Physik (in German) 94:59–86

Garthwaite AJ, Steudle E, Colmer TD (2006) Water uptake by roots of *Hordeum marinum*: formation of a barrier to radial O_2 loss does not affect root hydraulic conductivity. J Exp Bot 57:655–664. https://doi.org/10.1093/jxb/erj055

Haling RE, Brown LK, Bengough AG, Valentine TA, White PJ, Young IM, George TS (2014) Root hair length and rhizosheath mass depend on soil porosity, strength and water content in barley genotypes. Planta 239:643–651. https://doi.org/10.1007/s00425-013-2002-1

Henry A, Cal AJ, Batoto TC, Torres RO, Serraj R (2012) Root attributes affecting water uptake of rice (*Oryza sativa*) under drought. J Exp Bot 63:4751–4763. https://doi.org/10.1093/jxb/ers150

Hepworth C, Doheny-Adams T, Hunt L, Cameron DD, Gray JE (2015) Manipulating stomatal density enhances drought tolerance without deleterious effect on nutrient uptake. New Phytol 208:336–341. https://doi.org/10.1111/nph.13598

Hoegh-Guldberg O, Jacob D, Taylor M, Bindi M, Brown S, Camilloni I, Diedhiou A, Djalante R, Ebi KL, Engelbrecht F, Guiot J, Hijioka Y, Mehrotra S, Payne A, Seneviratne SI, Thomas A, Warren R, Zhou G (2018) Impacts of 1.5°C Global Warming on Natural and Human Systems. In: Masson-Delmotte PZV, Pörtner H-O, Roberts JSD, Shukla PR, Pirani A, Moufouma-Okia W, Péan C, Pidcock R, Connors S, Matthews JBR, Chen Y, Zhou X, Gomis MI, Lonnoy E, Maycock T, Tignor M, Waterfield T (eds) Global Warming of 15°C. IPCC

Jensen CR, Luxmoore RJ, Vangundy SD, Stolzy LH (1969) Root air space measurements by a pycnometer method 1. Agron J 61:474–475. https://doi.org/10.2134/agronj1969.00021962006100030045x

Jimenez JC, Clode PL, Signorelli S, Veneklaas EJ, Colmer TD, Kotula L (2021) The barrier to radial oxygen loss impedes the apoplastic entry of iron into the roots of *Urochloa humidicola*. J Exp Bot 72:3279–3293. https://doi.org/10.1093/jxb/erab043

Klein SP, Schneider HM, Perkins AC, Brown KM, Lynch JP (2020) Multiple integrated root phenotypes are associated with improved drought tolerance. Plant Physiol 183:1011–1025. https://doi.org/10.1104/pp.20.00211

Knutzen F, Meier IC, Leuschner C (2015) Does reduced precipitation trigger physiological and morphological drought adaptations in European beech (*Fagus sylvatica L.*)? Comparing provenances across a precipitation gradient. Tree Physiol 35:949–963. https://doi.org/10.1093/treephys/tpv057

Kotula L, Ranathunge K, Schreiber L, Steudle E (2009a) Functional and chemical comparison of apoplastic barriers to radial oxygen loss in roots of rice (*Oryza sativa* L.) grown in aerated or deoxygenated solution. J Exp Bot 60:2155–2167. https://doi.org/10.1093/jxb/erp089

Kotula L, Ranathunge K, Steudle E (2009b) Apoplastic barriers effectively block oxygen permeability across outer cell layers of rice roots under deoxygenated conditions: roles of apoplastic pores and of respiration. New Phytol 184:909–917. https://doi.org/10.1111/j.1469-8137.2009.03021.x

Kulichikhin K, Yamauchi T, Watanabe K, Nakazono M (2014) Biochemical and molecular characterization of rice (*Oryza sativa L.*) roots forming a barrier to radial oxygen loss. Plant Cell Environ 37:2406–2420. https://doi.org/10.1111/pce.12294

Leng G, Hall J (2019) Crop yield sensitivity of global major agricultural countries to droughts and the projected changes in the future. Sci Total Environ 654:811–821. https://doi.org/10.1016/j.scitotenv.2018.10.434

Lynch JP (2007) Roots of the second green revolution. Aust J Bot 55:493–512. https://doi.org/10.1071/bt06118

Lynch JP (2018) Rightsizing root phenotypes for drought resistance. J Exp Bot 69:3279–3292. https://doi.org/10.1093/jxb/ery048

Lynch JP, Chimungu JG, Brown KM (2014) Root anatomical phenes associated with water acquisition from drying soil: targets for crop improvement. J Exp Bot 65:6155–6166. https://doi.org/10.1093/jxb/eru162

Lynch JP, Strock CF, Schneider HM, Sidhu JS, Ajmera IB, Galindo-Castañeda T, Klein SP, Hanlon MT (2021) Root anatomy and soil resource capture. Plant Soil 466:21–63. https://doi.org/10.1007/s11104-021-05010-y

Mano Y, Omori F, Takamizo T, Kindiger B, Bird RM, Loaisiga CH (2006) Variation for root aerenchyma formation in flooded and non-flooded maize and teosinte seedlings. Plant Soil 281:269–279. https://doi.org/10.1007/s11104-005-4268-y

Mongon J, Konnerup D, Colmer TD, Rerkasem B (2014) Responses of rice to Fe^{2+} in aerated and stagnant conditions: growth, root porosity and radial oxygen loss barrier. Funct Plant Biol 41:922–929. https://doi.org/10.1071/FP13359

Nestler J, Keyes SD, Wissuwa M (2016) Root hair formation in rice (*Oryza sativa* L.) differs between root types and is altered in artificial growth conditions. J Exp Bot 67:3699–3708. https://doi.org/10.1093/jxb/erw115

Ouyang W, Yin X, Yang J, Struik PC (2020) Comparisons with wheat reveal root anatomical and histochemical constraints of rice under water-deficit stress. Plant Soil 452:547–568. https://doi.org/10.1007/s11104-020-04581-6

Pedersen O, Nakayama Y, Yasue H, Kurokawa Y, Takahashi H, Floytrup HA, Omori F, Mano Y, Colmer DT, Nakazono M (2021a) Lateral roots, in addition to adventitious roots, form a barrier to radial oxygen loss in *Zea nicaraguensis* and a chromosome segment introgression line in maize. New Phytol 229:94–105. https://doi.org/10.1111/nph.16452

Pedersen O, Sauter M, Colmer TD, Nakazono M (2021b) Regulation of root adaptive anatomical and morphological traits during low soil oxygen. New Phytol 229:42–49. https://doi.org/10.1111/nph.16375

Peralta Ogorek LL, Pellegrini E, Pedersen O (2021) Novel functions of the root barrier to radial oxygen loss - radial diffusion resistance to H_2 and water vapour. New Phytol 231:1365–1376. https://doi.org/10.1111/nph.17474

Ponnamperuma FN (1979) IR42: a rice type for small farmers of south and southeast Asia. 707 IRRI research paper series 44:1–10

Ranathunge K, Kotula L, Steudle E, Lafitte R (2004) Water permeability and reflection coefficient of the outer part of young rice roots are differently affected by closure of water channels (aquaporins) or blockage of apoplastic pores. J Exp Bot 55:433–447. https://doi.org/10.1093/jxb/erh041

Ray DK, Gerber JS, MacDonald GK, West PC (2015) Climate variation explains a third of global crop yield variability. Nature Communcations 6:5989. https://doi.org/10.1038/ncomms6989

Sanderson PL, Armstrong W (1980) The responses of conifers to some of the adverse factors associated with waterlogged soils. New Phytol 85:351–362. https://doi.org/10.1111/j.1469-8137.1980.tb03173.x

Schreiber L, Franke R, Hartmann KD, Ranathunge K, Steudle E (2005) The chemical composition of suberin in apoplastic barriers affects radial hydraulic conductivity differently in the roots of rice (*Oryza sativa* L. cv. IR64) and corn (*Zea mays* L. cv. Helix). J Exp Bot 56:1427–1436. https://doi.org/10.1093/jxb/eri144

Shiono K, Ogawa S, Yamazaki S, Isoda H, Fujimura T, Nakazono M, Colmer TD (2011) Contrasting dynamics of radial O$_2$-loss barrier induction and aerenchyma formation in rice roots of two lengths. Ann Bot 107:89–99. https://doi.org/10.1093/aob/mcq221

Soukup A, Armstrong W, Schreiber L, Franke R, Votrubova O (2007) Apoplastic barriers to radial oxygen loss and solute penetration: a chemical and functional comparison of the exodermis of two wetland species, *Phragmites australis* and *Glyceria maxima*. New Phytol 173:264–278. https://doi.org/10.1111/j.1469-8137.2006.01907.x

Stasovski E, Peterson CA (1993) Effects of drought and subsequent rehydration on the structure, vitality, and permeability of *Allium cepa* adventitious roots. Can J Bot-Revue Canadienne de Botanique 71:700–707. https://doi.org/10.1139/b93-080

Taleisnik E, Peyrano G, Cordoba A, Arlas C (1999) Water retention capacity in root segments differing in the degree of exodermis development. Ann Bot 83:19–27. https://doi.org/10.1006/anbo.1998.0781

Toulotte JM, Pantazopoulou CK, Sanclemente MA, Voesenek LACJ, Sasidharan R (2022) Water stress resilient cereal crops: Lessons from wild relatives. J Integr Plant Biol 64:412–430. https://doi.org/10.1111/jipb.13222

Truskey GA, Yuan F, Katz DF (2010) Transport phenomena in biological systems. Pearson New Jersey, New Jersey

Wiengweera A, Greenway H, Thomson CJ (1997) The use of agar nutrient solution to simulate lack of convection in waterlogged soils. Ann Bot 80:115–123. https://doi.org/10.1006/anbo.1996.0405

Wrońska-Wałach D, Sobucki M, Buchwał A, Gorczyca E, Korpak J, Wałdykowski P, Gärtner H (2016) Quantitative analysis of ring growth in spruce roots and its application towards a more precise dating. Dendrochronologia 38:61–71. https://doi.org/10.1016/j.dendro.2016.03.009

Yamauchi T, Shimamura S, Nakazono M, Mochizuki T (2013) Aerenchyma formation in crop species: A review. Field Crop Res 152:8–16. https://doi.org/10.1016/j.fcr.2012.12.008

Yamauchi T, Abe F, Tsutsumi N, Nakazono M (2019) Root cortex provides a venue for gas-space formation and is essential for plant adaptation to waterlogging. Front Plant Sci 10:259. https://doi.org/10.3389/fpls.2019.00259

Yamauchi T, Noshita K, Tsutsumi N (2021a) Climate-smart crops: key root anatomical traits that confer flooding tolerance. Breed Sci 71:51–61. https://doi.org/10.1270/jsbbs.20119

Yamauchi T, Pedersen O, Nakazono M, Tsutsumi N (2021b) Key root traits of Poaceae for adaptation to soil water gradients. New Phytol 229:3133–3140. https://doi.org/10.1111/nph.17093

Yang X, Li Y, Ren B, Ding L, Gao C, Shen Q, Guo S (2012) Drought-induced root aerenchyma formation restricts water uptake in rice seedlings supplied with nitrate. Plant Cell Physiol 53:495–504. https://doi.org/10.1093/pcp/pcs003

Yonis BO, del Carpio DP, Wolfe M, Jannink JL, Kulakow P, Rabbi I (2020) Improving root characterisation for genomic prediction in cassava. Sci Rep 10:8003. https://doi.org/10.1038/s41598-020-64963-9

Zhu J, Brown KM, Lynch JP (2010) Root cortical aerenchyma improves the drought tolerance of maize (*Zea mays* L.). Plant Cell Environ 33:740–749. https://doi.org/10.1111/j.1365-3040.2009.02099.x